Geomechanics and Engineering, *Vol. 9, No. 3 (2015) 287-311*
DOI: http://dx.doi.org/10.12989/gae.2015.9.3.287

The bearing capacity of square footings on a sand layer overlying clay

Erdal Uncuoğlu *

Civil Engineering Department, Erciyes University, 38039, Talas/Kayseri, Turkey

(*Received September 03, 2014, Revised January 29, 2015, Accepted April 21, 2015*)

Abstract. The ultimate bearing capacity and failure mechanism of square footings resting on a sand layer over clay soil have been investigated numerically by performing a series of three-dimensional non-linear finite element analyses. The parameters investigated are the thickness of upper sand layer, strength of sand, undrained shear strength of lower clay and surcharge effect. The results obtained from finite element analyses were compared with those from previous design methods based on limit equilibrium approach. The results proved that the parameters investigated had considerable effect on the ultimate bearing capacity and failure mechanism occurring. It was also shown that the thickness of upper sand layer, the undrained shear strength of lower clay and the strength of sand are the most important parameters affecting the type of failure will occur. The value of the ultimate bearing capacity could be significantly different depending on the limit equilibrium method used.

Keywords: square footing; bearing capacity; layered soils; finite element; numerical analysis

1. Introduction

The bearing capacity calculation is one of the most significant problems in foundation design. A common approach to estimate the bearing capacity of a vertically loaded footing placed on the surface of a homogeneous soil is the use of conventional Terzaghi bearing capacity theory (Terzaghi 1943).

Terzaghi bearing capacity theory is applicable to level strip footings resting on or near a level ground surface where the depth of the foundation is comparable to the foundation width. Also, theory assumes that bearing stratum is homogeneous and semi-infinite. The bearing capacity of three-dimensional footings such as square and rectangular shaped are predicted by applying empirical shape factors to basic equation developed for the plain-strain condition.

In reality, the subsoil profile often consists of distinct soil layers. Each layer may be assumed homogeneous in itself although the strength parameters of adjacent layers are quite different from each other. If the thickness of the top layer is less than the foundation width the failure surface will extent towards to bottom soil layers. In such case, any soil layers within the depth of failure surface would be expected to influence the bearing capacity. Therefore, conventional bearing capacity theory may not be appropriate to predict the failure loads.

*Corresponding author, Ph.D., E-mail: erdalu@erciyes.edu.tr

http://www.techno-press.org/?journal=gae&subpage=7 ISSN: 2005-307X (Print), 2092-6219 (Online)

Shallow foundations are sometimes located on the surface of a soil consisting of a uniform sand layer with limited thickness overlying a thick homogeneous bed of clay. In practice, the bearing capacity of foundations on soft clay is often improved by engineered granular fill layers.

Likewise, in road constructions, a compacted fill layer is used to spread the loads to underlying soft layers applied by vehicles. On the other hand, if a layer has a good bearing capacity does not exist at a shallow level, an evaluation of the possibility of relatively thin dense sand placed at shallow depths could be required to consider as a bearing capacity in the foundation design.

To evaluate the effect of soil layering on the bearing capacity is an important issue for the design of foundation resting on layered soil profile. The majority of the studies existing in the literature have been performed for the case of strip footing (Yamaguchi 1963, Yamaguchi and Terashi 1971, Meyerhof 1974, Purushothamaraj *et al*. 1974, Hanna and Meyerhof 1980, Hanna 1981, Baglioni *et al*. 1982, Kraft and Helfrich 1983, Florkiewicz 1989, Michalowski and Shi 1995, Burd and Frydman 1997, Kenny and Andrawes 1997, Okamura *et al*. 1997, 1998, Merifield *et al*. 1999, Shiau *et al*. 2003, Yamamoto and Kim 2004, Yuan and Luan 2005, Merifield and Nguyen 2006, Akpila 2007, Huang and Qin 2009, Bandini and Pham 2011, Benmebarek *et al*. 2012). On the contrary, few experimental, analytical and numerical studies of the bearing capacity of square footings have been carried out (Gourvenec *et al*. 2006, Merifield and Nguyen 2006, Yu *et al*. 2011). The studies for the square footings mentioned above have been performed in the case of two-layered clays.

No exact solution exists for the problem of surface square footings placed on a uniform sand layer overlying a clay layer. Therefore, the bearing capacity and failure mechanism of such non-homogeneous soil profiles still remain unclear (Yamamoto and Kim 2004, Gourvenec *et al*. 2006, Merifield and Nguyen 2006).

In this paper, three-dimensional non-linear numerical analyses by finite element method have been performed to investigate the effects of various parameters on the bearing capacity and failure mechanism of a square footing placed on the surface of a soil consisting of a uniform sand layer overlying a thick homogeneous bed of clay. The parameters considered in the numerical analyses are the thickness of upper sand layer, the strength of sand, the undrained shear strength of lower clay layer and surcharge effect. In addition, the developments of failure types depending on the thickness of upper sand layer and strength parameters of adjacent layers have been investigated. Considering the parameters discussed in the study, the changing in the resulting plastic failure zones were examined. However, the ultimate bearing capacity of square footings in two-layer foundation soils predicted by finite element analyses were compared with the results obtained from design methods proposed by Meyerhof (1974) and Okamura *et al*. (1998). The various parameters and dimensionless groups influenced the bearing capacity of layered subsoil have been defined to specify the parametric studies.

2. Definition of the problem

The analytical conditions of the three-dimensional bearing capacity problem considered in this paper are illustrated in Fig. 1. A square footing of width B rests upon an upper sand layer has a thickness of H. This sand layer is underlain by a deep bed of clay which has a thickness of 8B-H.

In the bearing capacity calculations, unit weights of γ = 15.03 kN/m^3 and γ = 17.06 kN/m^3 for the sand layer were used for the loose and dense packings, respectively. The values of the internal friction angles were ϕ' = 38° and ϕ' = 44° for the cases of loose and dense sand conditions,

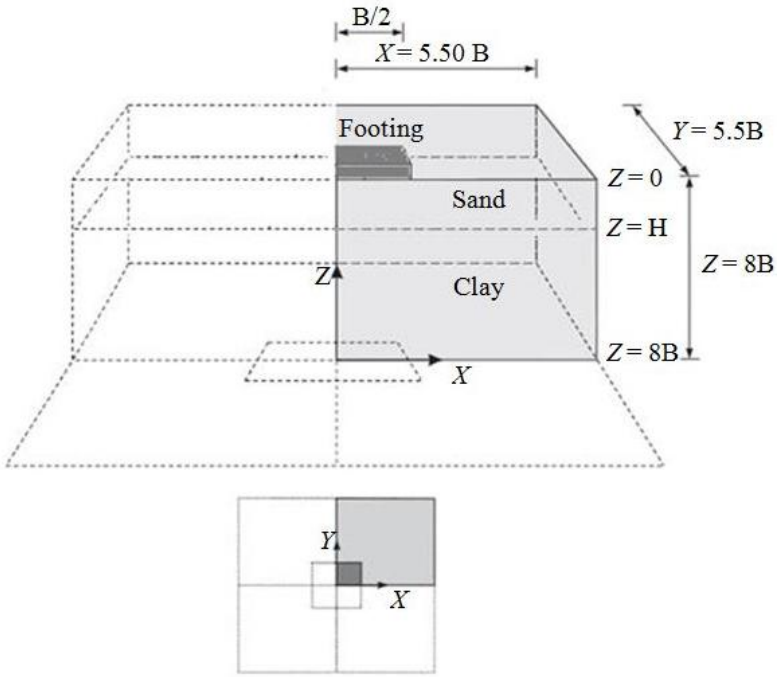

Fig. 1 Problem definition

respectively. The undrained shear strength values chosen for the clay layer depending on the consistence were c_u = 7.50, 15.03, 30.06 and 45.09 kN/m². Each layer was assumed to be homogeneous. The clay was assumed to be incompressible. The condition considered is intended to represent undrained behavior of a fully saturated fine grained material subjected to a period of loading sufficiently short. To avoid complications, Plaxis advised to enter at least a small value for cohesion (c > 0.20 kPa) parameter in case of cohesionless sands. Since only short-term stability of the square footing was considered, the sand layer was assumed to be fully drained while the clay layer was undrained. Symmetry has been exploited for the three-dimensional finite element (FE) analyses. Therefore, only one-quarter of the problem geometry has been modelled.

The ultimate bearing capacity of the two-layer foundation problem can be expressed as the function of dimensionless quantities given below (Michalowski and Shi 1995, Shiau *et al*. 2003).

$$\frac{p}{\gamma B} = f\left(\frac{H}{B}, \frac{c_u}{\gamma B}, \frac{q}{\gamma B}, \phi'\right) \tag{1}$$

Where;
p; average limit pressure under the footing,
B; footing width,
H; thickness of the upper sand layer,
c_u; undrained shear strength of the lower clay layer,
γ; the unit weight of the sand,
ϕ'; internal friction angle of the sand,
q; surcharge load at the base level of the footing.

The bearing capacity is independent of the clay unit weight because of the assumed undrained behavior of the clay layer (Michalowski and Shi 1995, Merifield *et al*. 1999). In this study, three-dimensional non-linear FE analyses have been performed for the problems where H/B ranges from 0.25 to 3.00 and c_u/γB values vary from 0.50 to 3.00. These cover most problems of practical interest.

3. Finite element modelling details

All the finite element (FE) calculations were carried out using the software PLAXIS 3D (2012). The program is formulated using the displacement method and it uses the constitutive models based on plasticity theory.

Finite element modelling details of square footing is shown in Fig. 2. The side boundaries of the mesh extend 5.5B from the footing center while the bottom boundary is far 8B from the ground surface. The selected mesh dimensions were placed enough to ensure that the zones of plastic failure and the observed displacement field were contained within the model boundaries at all of the analyses. Plaxis automatically imposes a set of general fixities to the boundaries of the geometry model. Zero-displacement boundary conditions prevent out-of-plane displacements of the vertical boundaries and bottom boundary of the mesh is fixed in all three coordinate directions. The mesh density including number of nodes, number of elements and average element size was defined after performing a series of trial analyses with several meshes of increasing refinement using the model dimensions given above. The analyses have been carried out until no significant changes were observed with further refinement. The medium mesh density was selected at the end of the analyses. The selected mesh density is also refined beneath the footing area. The average element sizes in all cases analyzed were approximately same. The mesh shown in Fig. 2 comprises 8894 elements and 13735 nodes. The PLAXIS 3D (2012) program allows for a fully automatic generation of FE meshes. The basic soil elements of the 3D mesh are the 10-node tetrahedral elements. In addition, 6-node plate element is used to simulate the behavior of plates. Moreover, 12-node interface elements are used to simulate soil-structure interaction behavior.

In this study, the sand layer was treated as a linear elastic-perfectly plastic frictional material and the clay was assumed to be linear elastic-perfectly plastic cohesive material. Mohr-Coulomb (MC) material model was used to simulate non-linear soil layers behavior because of its simplicity, reasonable number of model parameters and reasonable accuracy in modelling the bearing capacity problem of footings. If it is assumed that, the mobilized friction angle within the failure zone corresponds to the peak value, it would be appropriate to set the friction angle of sand, ϕ', as equal to peak friction angle, ϕ'_P (Burd and Frydman 1997). Also, the behavior of sand layer would be expected to be influenced by its dilation angle. The angle of dilation, ψ, is known to be related to the peak friction angle, ϕ'_p and the critical state friction angle, ϕ'_c of sand. To obtain the suitable values of the ψ for use in the FE calculations following formula recommended by PLAXIS was used.

$$\psi \approx \phi'_p - 30° \tag{2}$$

The MC model has a fixed yield surface and yield surface is not affected by plastic straining. For MC type yield functions, the theory of plasticity overestimates dilatancy. Therefore, in addition to the yield function, *f*, a plastic potential function, *g*, is introduced. The plastic potential function contains the parameter of dilation angle which is required to model positive plastic

volumetric strain increments. The case $g \neq f$ is denoted as non-associated plasticity. In the non-associated flow rule ($\psi < \phi'$), plastic potential function is assumed to take a similar form to that of the yield function but ϕ' replaced by ψ.

Different modelling schemes are possible in PLAXIS 3D (2012) to model undrained behavior of clay. In this study, undrained clay behavior was modelled using the option of effective stress analysis with undrained strength parameters. This option enables modelling undrained behavior using effective parameters for stiffness (Young's modulus, E' and poisson ratio, ν') and undrained strength parameters ($\phi' = \phi_u = 0°$ and $c_u = s_u$). The elastic behavior was described by a poisson ratio $\nu' = 0.33$ and a ratio of undrained Young's modulus to undrained shear strength of $E_u/c_u = 500$. In this type undrained analyses, In order to ensure realistic computational results, the bulk modulus of the water must be high compared with the bulk modulus of the soil skeleton. This condition is sufficiently ensured by requiring $\nu' < 0.35$. On the other hand, the effective value of Young's moduli was calculated based on the following equation proposed by PLAXIS. The undrained shear strength of clay layer has been assumed as constant with depth for the analyses performed within the scope of this paper.

$$E' = \frac{2(1+\nu')}{3} E_u \tag{3}$$

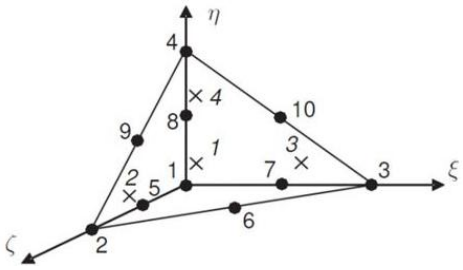

(a) 3D soil elements

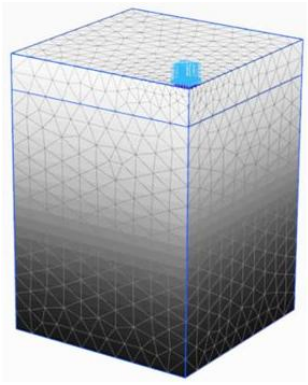

(b) 3D mesh of the numerical model

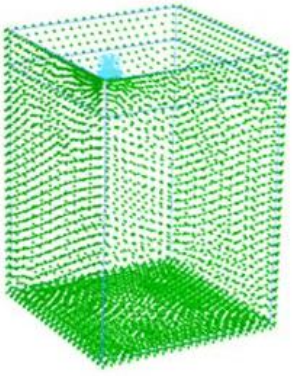

(c) Boundary conditions

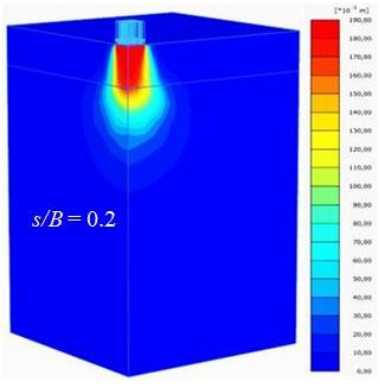

(d) Displacement field

Fig. 2 Finite element modelling details

In all the FE analyses, the footing was assumed to be rigid and perfectly rough. Footing was modelled by plate element. The roughness of the footing base was considered taking the value of R_{inter} coefficient equal to 1. R_{inter} value defines the interface behavior depending on the soil strength parameters (i.e., c, ϕ and ψ). In order to obtain load-displacement relationship as shown in Fig. 3, loading was achieved by applying the uniform distributed vertical pressure over the footing area. Load-displacement relationships can be obtained completely using the displacement finite element method. The footing behaviour and failure mechanism can be understood more clearly by this way. In order to consider more realistic stress conditions in the soil, FE calculations can be divided into several sequential calculation phases. Many analysis problems in geotechnical engineering require specification of initial stresses. The initial stresses in a soil body are influenced by the weight of the material and history of its formation. This stress state is usually represented by an initial vertical effective stress. The initial horizontal effective stress is related to the initial vertical effective stress by the coefficient of lateral earth pressure at-rest, K_0. For the Mohr-Coulomb model, K_0 value is obtained based on Jaky's formula given by $K_0 = 1 - \sin\phi'$ (Jaky 1944). At the end of the initial stress generation, the full soil weight activated. The vertical displacement of the footing is generated in the plastic calculation phase. The deformations occurred in the initial stress generation are set to zero beginning of the plastic calculation phase. Therefore, the total displacement in the plastic calculation can be defined as the settlement occurring in the loading stage. In the plastic calculation, the total load value that is to be applied is specified. Plaxis has an automatic load stepping procedure for the solution of non-linear plasticity problems. The load value is increased step by step for each iteration, and the displacement value corresponds to the loads are obtained. The calculation terminates when the specified load level is reached or when soil body is collapsed. Then, load-displacement curves are obtained. End of the calculation steps, ultimate bearing capacity can be evaluated observing the load-displacement response. The properties of the soil layers and footing material used in the analyses are summarized in Table 1.

4. Results and discussions

The occurrence of failure mechanism and the bearing capacity of square footings located in a sand stratum of limited thickness on a deep bed of clay depend on some parameters such as the thickness of upper sand layer (H), the undrained shear strength of clay (c_u), the effective internal friction of sand (ϕ'), the deformation characteristics of layers and the surcharge pressure (q).

To investigate the effects of these parameters on the bearing capacity behavior of square footings a series of 3D non-linear FE analyses were performed considering the different values of H/B, c_u/γB, ϕ' and q/γB. Footing width equal to B = 1.0 m. was used in the analyses. In the FE simulations, the different values of H/B ratio ranging from 0.25 to 3.0 were used while c_u/γB values were selected in the range of 0.50 to 3.0. However, two ϕ' (ϕ' = 38° and 44°) and four surcharge (q/γB = 0, 0.50, 1.0 and 2.0) values were considered.

The characteristics of the load-settlement curves essentially depend on the failure type such as general, local or punching shear failure. Since local and punching shear failure may occur in the layered soil conditions there is no obvious peak value in the load-settlement curve. In load-defined finite element (FE) analysis of footings subjected to vertical load, to find a point at which overall failure can be assumed to occur is very difficult. (Taiebat and Carter 2000, Yuan and Luan 2005).

There are different methods for determining the ultimate bearing capacity, q_u, from load-settlement curves in the literature. One of them is to define the q_u as the load corresponding to a

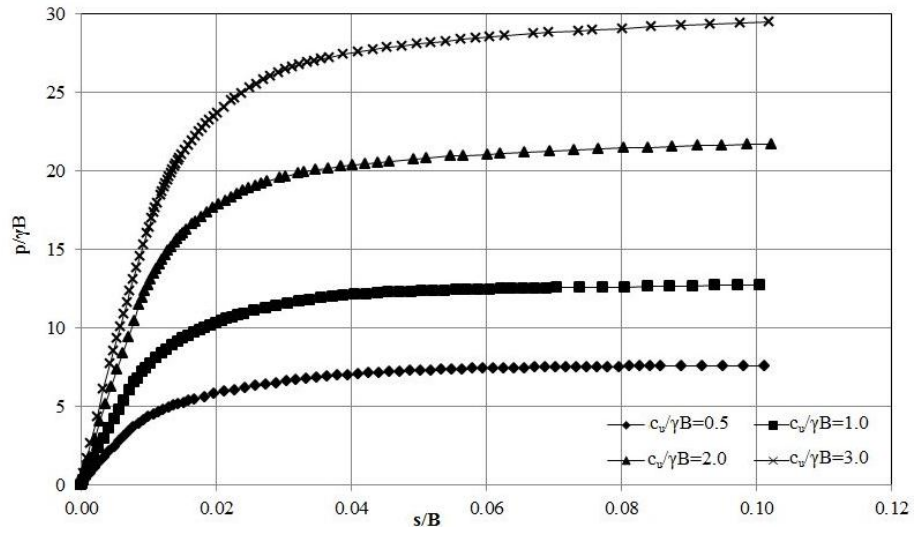

Fig. 3 Load-displacement curves obtained for the ratio of H/B = 0.50 ($q/\gamma B = 0$, $\phi' = 38°$)

settlement ratio equals to s/B = 0.1. According to the full-scaled tests conducted in the Laboratoires des Ponts et Chaussees (LPC), the bearing capacity has been consistently defined as the load corresponding to a vertical displacement equal to 10% of the footing width (Amar *et al*. 1994, Lavasan and Ghazari 2012). Briaud and Jeanjean (1994), Cerato (2005) and Cerato and Lutenegger (2007) also adopted this criteria to define the ultimate bearing capacity because of its simplicity consistency for different size foundations and may be actually close to the average soil strain at failure. In the present study, the footing unit load q_b corresponding to the vertical displacement equal to 10% of the footing width was defined as the ultimate bearing capacity, q_u. This failure criterion is valid for all of the analyses presented in this paper.

Fig. 4 shows the relationships between normalized bearing capacity $p/\gamma B$ and H/B ratio for different $c_u/\gamma B$ values. As shown in Fig. 4, $p/\gamma B$ value of the layered soil increases with increasing thickness of upper sand layer until it reaches that of uniform sand. The value of $p/\gamma B$ obtained in the case of uniform sand is an upper limit for the normalized bearing capacity of sand layer overlying clay. The value of H/B in which $p/\gamma B$ of layered soil reaches that of uniform sand is refer as to $H/B_{critical}$. It can be said that the failure zone is confined entirely to the upper sand layer for the H/B values greater than $H/B_{critical}$. Fig. 5 illustrates the plastic failure zones for various values of H/B with $\phi' = 38°$, $c_u/\gamma B = 2.0$ and $q/\gamma B = 0$. These plots clearly demonstrate the improved bearing capacity. As H/B ratio increases, the proportion of the failure mechanism in the upper sand layer increases. Fig. 6 shows the deformation diagrams obtained from analyses for different cases. From Fig. 6, it is seen that the value of $H/B_{critical}$ is also varies depending on the undrained shear strength of lower clay layer. For the cases with H/B smaller than $H/B_{critical}$, $p/\gamma B$ increases with increasing $c_u/\gamma B$. The relationship between $p/\gamma B$ and $c_u/\gamma B$ is approximately linear in the cases of $H/B \leq 1$ while it is not linear for $H/B > 1$ (Fig. 7). The critical depth, $H/B_{critical}$, is not a constant value for the layered soils. It changes depending on both the strengths of upper sand layer and lower clay layer. Thus, for the cases of $c_u/\gamma B \leq 2.0$, the value of H/B ratio is equal to 3 while for the cases of $c_u/\gamma B > 2$ it is approximately $H/B \geq 1.50$. $H/B_{critical}$ decreases with increasing value of $c_u/\gamma B$. The shape of the failure zones formed by plastic stress points undergoes a change based

on the combination of layers considered.

Fig. 5 illustrates the plastic failure zones for various values of H/B with $\phi' = 38°$, $c_u/\gamma B = 2.0$ and $q/\gamma B = 0$. These plots clearly demonstrate the improved bearing capacity. As H/B ratio increases, the proportion of the failure mechanism in the upper sand layer increases. Fig. 6 shows the deformation diagrams obtained from analyses for different cases. From Fig. 6, it is seen that

Table 1 The properties of the soil layers and footing material

	Sand properties	
	Loose condition	Dense condition
Peak friction angle, ϕ'_{peak} (°)	38	44
Cohesion, c' (kN/m²)	0.30	0.30
Unit weight, γ_{sand} (kN/m³)	15.03	17.06
Dilation angle, ψ (°)	8	14
Young's modulus, E' (kN/m²)	20600	30000
Poisson's ratio, ν'	0.30	0.30
	Clay properties	
Peak friction angle, ϕ'_{peak} (°)	$\phi' = \phi_u = 0°$	
Unit weight, γ_{clay} (kN/m³)	21.00	
Dilation angle, ψ (°)	0	
Poisson's ratio, ν'	0.33	
	Footing material properties	
Unit weight, $\gamma_{footing}$ (kN/m³)	24.00	
Young's modulus, $E_{footing}$ (kN/m²)	30×10^6	
Poisson's ratio, ν	0.15	
Material model	Linear Elastic (LE)	

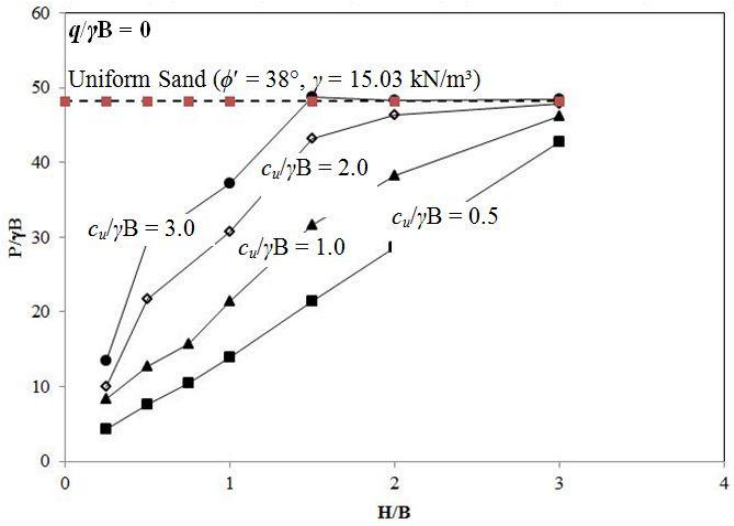

Fig. 4 Variation of the $p/\gamma B$ with H/B

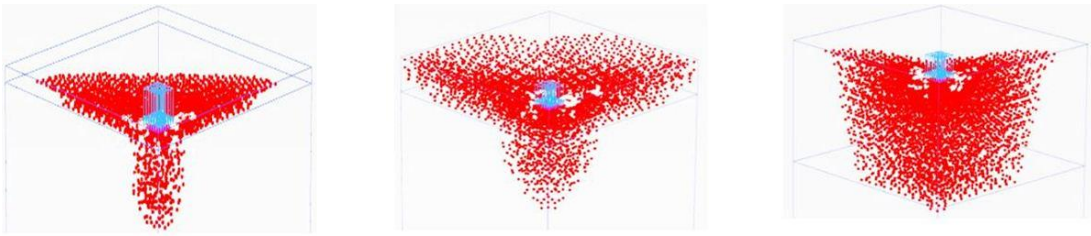

(a) (b) (c)

Fig. 5 The variation of plastic failure zones with H/B (ϕ' = 38°, $c_u/\gamma B$ = 2.0, $q/\gamma B$ = 0)

the value of $H/B_{critical}$ is also varies depending on the undrained shear strength of lower clay layer. For the cases with H/B smaller than $H/B_{critical}$, $p/\gamma B$ increases with increasing $c_u/\gamma B$. The relationship between $p/\gamma B$ and $c_u/\gamma B$ is approximately linear in the cases of H/B ≤ 1 while it is not linear for H/B > 1 (Fig. 7). The critical depth, $H/B_{critical}$, is not a constant value for the layered soils. It changes depending on both the strengths of upper sand layer and lower clay layer. Thus, for the cases of $c_u/\gamma B \leq 2.0$, the value of H/B ratio is equal to 3 while for the cases of $c_u/\gamma B > 2$ it is approximately H/B ≥ 1.50. $H/B_{critical}$ decreases with increasing value of $c_u/\gamma B$. The shape of the failure zones formed by plastic stress points undergoes a change based on the combination of layers considered.

At the ultimate load, the square footings rest on a sand layer overlying clay deposit can be subjected to failure in different ways such as full punching shear failure, partial punching shear failure and general shear failure. The thickness of the upper sand layer (H), the undrained shear strength (c_u) of lower clay and the strength of sand (ϕ') are the most important parameters affecting the type of failure will occur. The failure type has been defined as full punching shear failure for

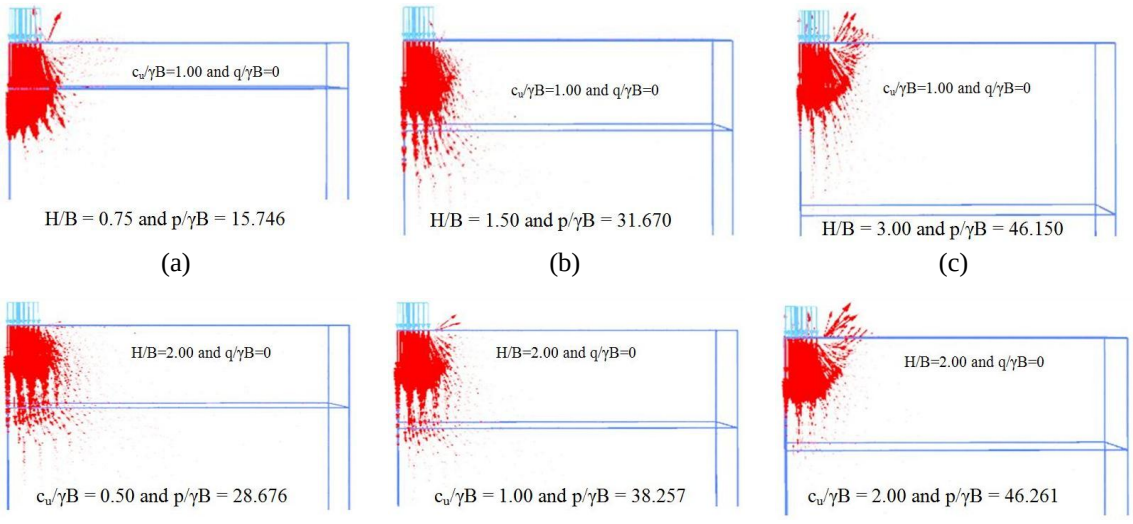

(a) (b) (c)

(d) (e) (f)

Fig. 6 Displacement fields obtained for different cases

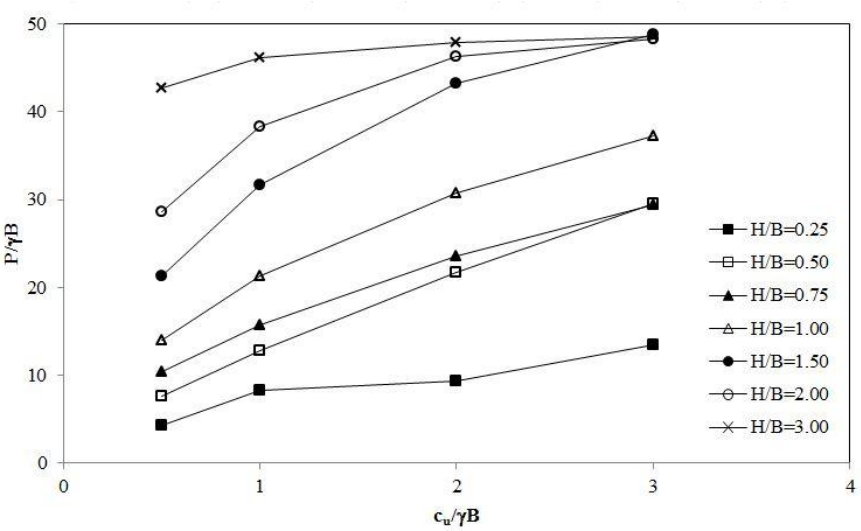

Fig. 7 Variation of $p/\gamma B$ with $c_u/\gamma B$ ($\phi' = 38°$, $q/\gamma B = 0$)

the normalized bearing capacities, $p/\gamma B$, up to 70% of the $p/\gamma B$ value estimated for the case of uniform sand condition. If the $p/\gamma B$ values are greater than or equal to the normalized bearing capacity calculated for the case of uniform sand, failure is generally caused by general shear failure.

If the upper sand layer is substantially stronger than the lower clay full punching shear failure through the top layer occurs. A soil mass of roughly truncated pyramidal shape between the footing base and the clay surface penetrates into the clay and a general shear takes place in the clay. The vertical separation of the sand block in the upper layer and then the punching of the block through to the bottom layer are seen clearly from Fig. 8(a). The mobilized angle of shearing resistance could be considerably less than the peak value at low values of shear strength ratio ($c_u/\gamma B$). So, the dominant parameter on the bearing capacity is the undrained shear strength of clay and the normalized bearing capacity, $p/\gamma B$, increases with increasing $c_u/\gamma B$.

The value of mobilized internal friction angle increases with increasing undrained shear strength of clay. As a result of this, failure type transforms from full punching shear failure to partial punching shear failure. As shown in Fig. 8(b) the separation of the sand block takes place along a surface inclined at angle α to vertical. However, the penetration of the sand block into clay tends to reduce significantly as the value of $c_u/\gamma B$ increases. As expected, the fraction of the failure mechanism confined to the sand layer increases. These observations may lead to a conclusion that the contribution of the upper sand layer to the bearing capacity increases and failure mechanism occurs under the combined effects of ϕ' and c_u.

In the uniform sand condition, it is assumed that the mobilized angle of internal friction is equal to peak value at failure. For the cases with H/B and $c_u/\gamma B$ greater than those of certain values, the layered soil profile exhibit bearing capacity behavior similar to that of uniform sand and the failure surface will be completely located in the upper sand layer. As seen in Fig. 8(c), the general shear dominates the failure behavior and penetration of the upper sand layer into underlying clay is not the case. The angle of separation surface with vertical increases in general shear failure compared to partial punching shear failure. As a result, heaving in the soil adjacent to the side of the footing

more remarkable. The parameter governing the bearing capacity behavior is the mobilized internal friction angle.

The extent and form of the failure mechanism is mainly depend on depth and strength of upper sand layer and undrained shear strength of lower clay. A series of finite element analyses have been performed to investigate the development of failure mechanism. In the analyses, load-settlement behaviors were extended up to a settlement level equal to 20% of the footing width to present that punching or local shear is indeed the failure mechanism. The development of the failure mechanisms are illustrated by deformed mesh and displacement diagrams in Fig. 8. As seen in Fig. 8, punching and local shears are indeed the failure mechanisms because of development of failure type are not affected from the amount of footing settlement.

Fig. 9 represents the failure type diagram created by examining the normalized bearing capacity values, displacement diagrams and plastic yielding zones obtained end of the analyses performed for different values of H/B (= 0.25, 0.50, 1.0, 1.50, 2.0 and 3.0), $c_u/\gamma B$ (= 0.50, 1.0, 2.0 and 3.0), ϕ' (= 38° and 44°) with $q/\gamma B = 0$. It can be said that increasing strength of upper sand layer increases the probability of punching shear type failure.

As the thickness of upper sand layer greater than the footing width it does not always mean that the failure zone is limited in the sand. As illustrated in Fig. 10, the failure mechanism may extent into the underlying clay depending on the undrained shear strength of clay. When the bearing capacity of a sand layer overlying clay reaches that of the uniform sand it becomes independent of the $c_u/\gamma B$ value.

The values of the vertical displacements obtained on the clay surface for $\phi' = 38°$ and $\phi' = 44°$ with different values of both H/B and $c_u/\gamma B$ are summarized in Table 2. As seen from Table 2, at

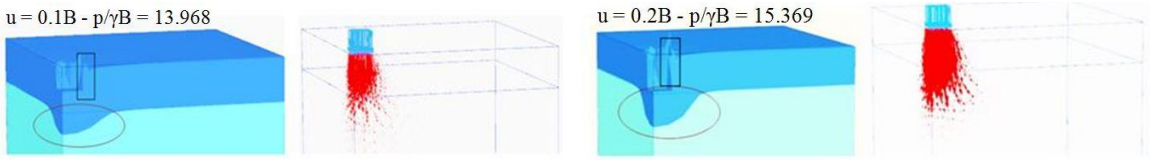

(a) H/B = 1.0, $c_u/\gamma B = 0.5$, $\phi' = 38°$, $q/\gamma B = 0$

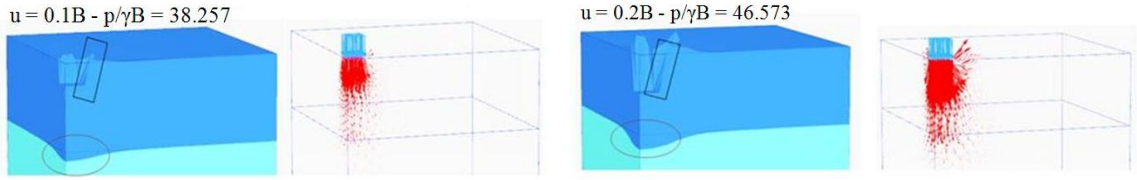

(b) H/B = 2.0, $c_u/\gamma B = 1.0$, $\phi' = 38°$, $q/\gamma B = 0$

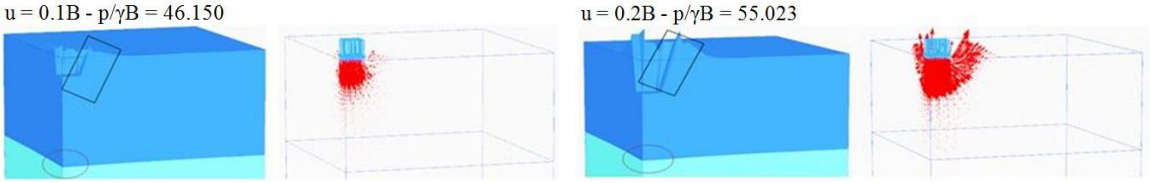

(b) H/B = 3.0, $c_u/\gamma B = 1.0$, $\phi' = 38°$, $q/\gamma B = 0$

Fig. 8 The types of failure mechanisms developed

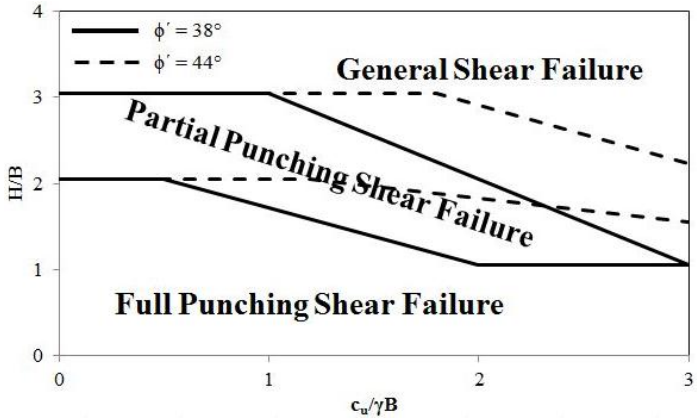

Fig. 9 The division among the full punching, partial punching and general shear failures

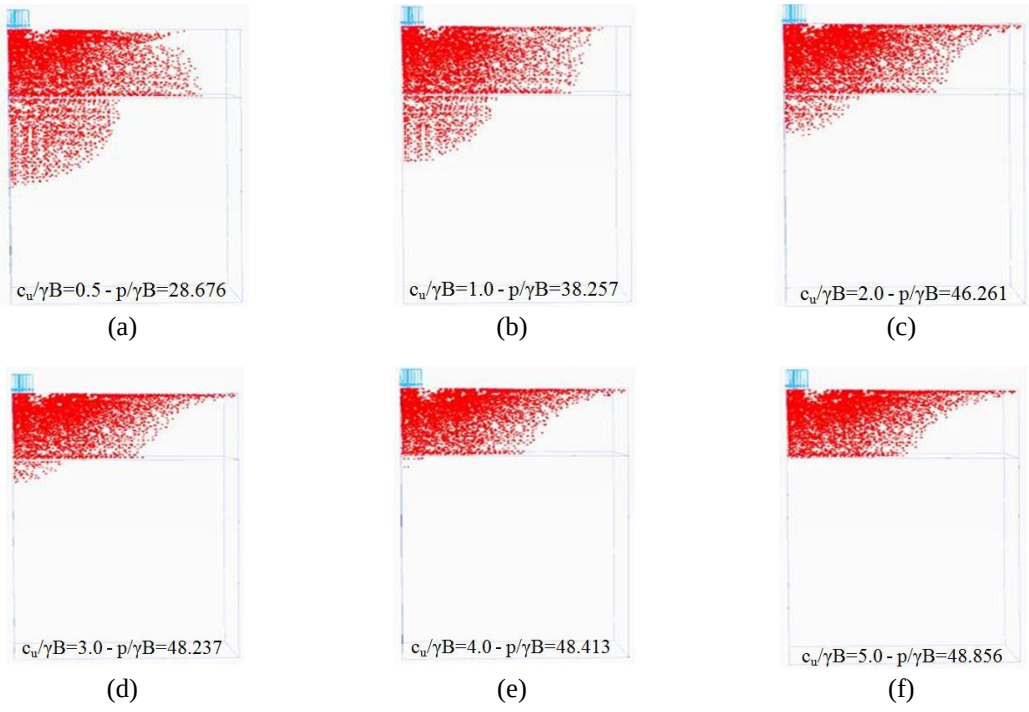

(a) (b) (c)

(d) (e) (f)

Fig. 10 The variation of plastic failure zones with $c_u/\gamma B$ (H/B = 2.0, $q/\gamma B$ = 0)

failure, the amount of vertical displacement occurred in the sand and clay layers are not equal to each other. The results obtained from the analyses performed for different values of H/B by keeping the $c_u/\gamma B$ constant indicate that the amount of the vertical displacement occurring in the sand layer, considering the total vertical displacement caused failure, increases with increasing H/B. Such that for $\phi' = 38°$ and H/B = 0.50, the vertical displacement observed in the sand layer is about 2% of the total vertical displacement while this ratio is approximately 90% in the case of H/B = 3.00. Likewise, in the case of $\phi' = 44°$, the vertical displacement observed in the sand layer

Table 2 Vertical displacement values obtained on the clay surface for the cases of $\phi' = 38°$ and $\phi' = 44°$

H/B	$c_u/\gamma B$	x	y	z	$u_{z\text{-}\phi'=38°}$ (*10^{-3} m)	$u_{z\text{-}\phi'=44°}$ (*10^{-3} m)
0.50	1.00	0	0	-0.50	-97.726	-96.223
1.00	1.00	0	0	-1.00	-88.231	-86.177
1.50	1.00	0	0	-1.50	-70.906	-79.562
2.00	1.00	0	0	-2.00	-40.046	-57.288
3.00	1.00	0	0	-3.00	-10.152	-27.610
1.00	0.50	0	0	-1.00	-95.895	-94.177
1.00	1.00	0	0	-1.00	-88.231	-86.177
1.00	2.00	0	0	-1.00	-79.199	-83.053
1.00	3.00	0	0	-1.00	-73.744	-77.630

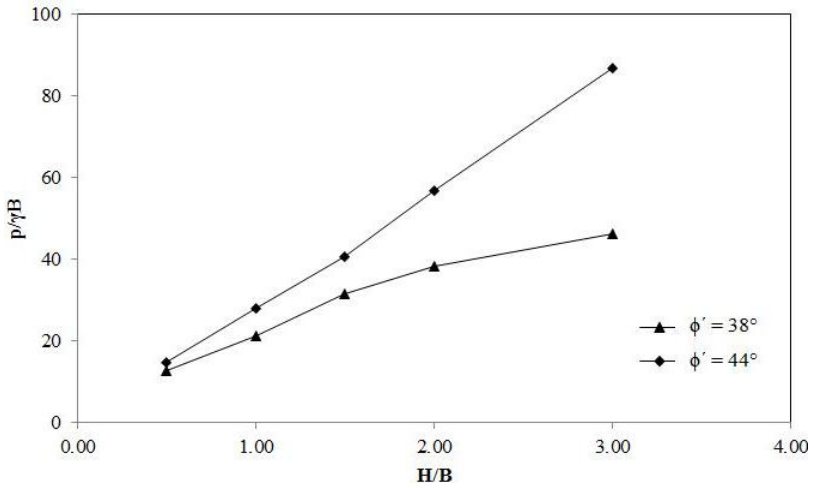

Fig. 11 The effect of the sand strength on the normalized bearing capacity ($c_u/\gamma B = 1.0$, $q/\gamma B = 0$)

are equal to 4% and 72% of the total vertical displacement for the cases of H/B = 0.50 and H/B = 3.00, respectively.

As a consequence of increasing amount of vertical displacements in the sand layer the value of the mobilized angle of shearing resistance approaches to the peak value and the bearing capacity of sand layer overlying clay increases. The value of mobilized angle of internal friction can be assumed as equal to peak value for the cases H/B > 2.0. However, since the vertical stress increment on the surface of clay layer decreases with increasing thickness of upper sand layer, the influence of clay layer on the bearing capacity and failure mechanism will be decreased with increasing H/B.

In the case of H/B = 0.50 with $c_u/\gamma B = 1.0$, the vertical displacements obtained on the clay surface are almost the same for $\phi' = 38°$ and $\phi' = 44°$. This observation is valid also for the case of H/B = 1.0 with $c_u/\gamma B = 1.0$. This result clearly indicates that failure occurs depending on the bearing capacity of lower clay layer and the strength of sand is not efficient on failure behavior for the cases of H/B $\leq$ 1.0. Increasing undrained shear strength of clay effects the deformation

Table 3 The effect of the sand strength on the bearing capacity

$\phi' = 38°$			$\phi' = 44°$			(%)
H/B	c_u/γB	p/γB	H/B	c_u/γB	P/γB	
0.50	1.00	12.775	0.50	1.00	14.652	14.700
1.00	1.00	21.342	1.00	1.00	28.019	31.280
1.50	1.00	31.670	1.50	1.00	40.797	28.820
2.00	1.00	38.257	2.00	1.00	56.858	48.622
3.00	1.00	46.150	3.00	1.00	86.795	88.070

behavior of sand. Such that since the penetration of the upper sand layer into clay gets difficult with increasing value of c_u/γB, the amount of compression occurred in the sand layer will increase. Consequently, as the lateral movements increase, resulting in an increase in mobilized internal friction angle. This lateral movement may not be sufficient for the maximum mobilization of the ϕ'.

As can be seen from Fig. 11, the effect of the sand strength on the bearing capacity is more remarkable for the H/B values which are close to or greater than the critical thickness of upper sand layer. As shown in Table 3, the rate of increment in normalized bearing capacity, p/γB, is equal to %15 in the case of H/B = 0.50, c_u/γB = 1.0 and q/γB = 0 as ϕ' is increased from 38° to 44°. For the same set of strength parameters but with H/B = 2.0 and H/B = 3.0, this ratio is equal to %49 and %88, respectively.

From Fig. 12, it is seen that as the H/B increases, the surcharge effect on the clay layer increases. The surcharge clearly suppresses the upward movement of clay and forces the plastic failure zone to be much wider and deeper mobilizing more of the available shear strength of clay and provides a positive contribution to the bearing capacity. This behavior is more remarkable for the cases in which the governing criterion for the bearing capacity is undrained shear strength of clay. However; similar behavior could not be observed for the cases with H/B ratios (H/B $\geq$ 1.50) in which the thickness of upper sand layer close to or greater than $H/B_{critical}$. In the latter case, bearing capacity increases depending on the size of plastic failure zones situated within the upper sand layer.

Fig. 13 presents the relationships between p/γB and c_u/γB obtained for the different values of ϕ' for the case where H/B = 1.0 and q/γB = 0. It is seen from Fig. 13 that p/γB increases with increasing c_u/γB in both cases. The p/γB values obtained from FE analyses performed for different values of c_u/γB keeping the H/B ratio constant as equal to 1.0 in the cases of $\phi' = 38°$ and $\phi' = 44°$ are summarized in Table 4. As shown in Table 4, the rate of increment in p/γB is equal to 29% in the case of c_u/γB = 0.50, H/B = 1.00 and q/γB = 0 as ϕ' is increased from 38° to 44° while this ratio is equal to 37% for the case of c_u/γB = 3.0. This fact implies that since the increasing undrained shear strength of clay increases the compressibility of the sand mass between the footing base and clay layer, it provides a positive contribution to the bearing capacity.

As illustrated in Fig. 14, the portion of the plastic failure zones occurring in the clay layer get much wider and deeper due to the increasing strength of sand. It is expected to occur punching shear failure for the cases with relatively limited upper layer thicknesses such as H/B = 0.50 and 1.0. On the other hand, increasing ϕ' in the upper sand layer giving rise to possibility of punching shear failure also with increasing H/B.

4.1 Comparison with predictions from previous design methods based on limit equilibrium approach

Some of the design methods based on limit equilibrium approach to predict the ultimate bearing capacity of footings on sand layer overlying clay are briefly summarized in the following.

The bearing capacity of a strip footing placed on soil surface is estimated using Punching Shear Model suggested by Meyerhof (1974). In this model, it is considered that a sand block with vertical sides is pushed together with footing into lower clay layer. In addition, it is assumed that the sand layer to be in a state of passive failure along vertical planes beneath the footing edges. The bearing capacity of footing is obtained from the equilibrium of forces acted on sand block. Meyerhof (1974) suggested the following equation to determine the bearing capacity of rectangular footings.

$$q_u = \left(1 + 0.2\frac{B}{L}\right) cN_c + \left(1 + \frac{B}{L}\right) \gamma H^2 (1 + 2D/H) K_S \, tan\emptyset/B + \gamma D \tag{4}$$

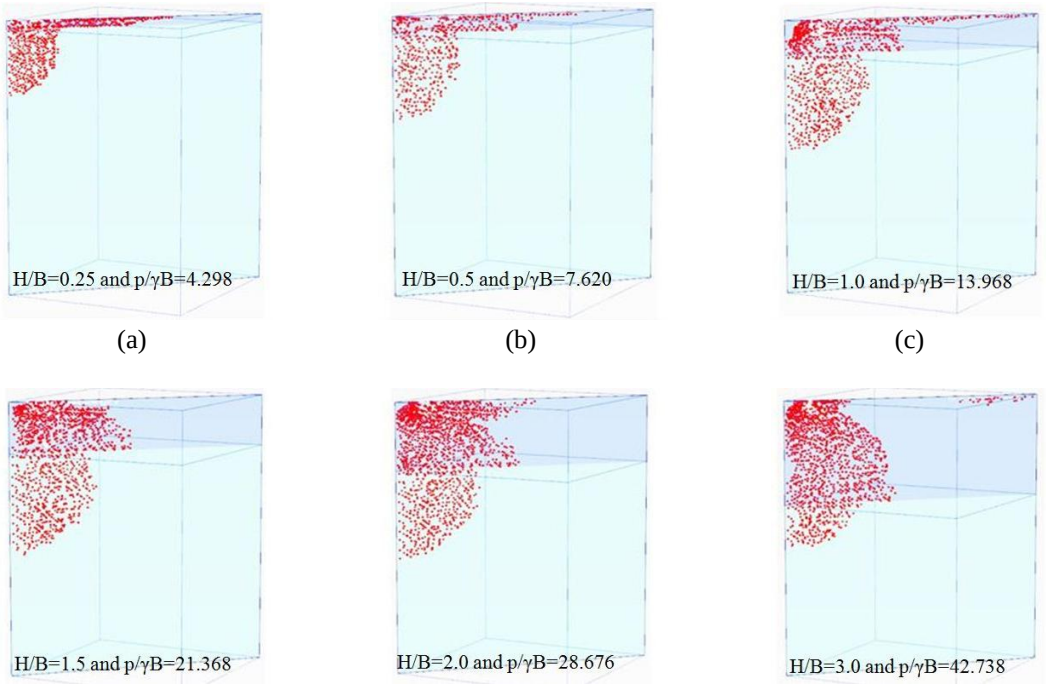

(a) (b) (c)

(d) (e) (f)

Fig. 12 The variation of the plastic yielding zones with H/B ratio ($c_u/\gamma B = 0.5$, $q/\gamma B = 0$)

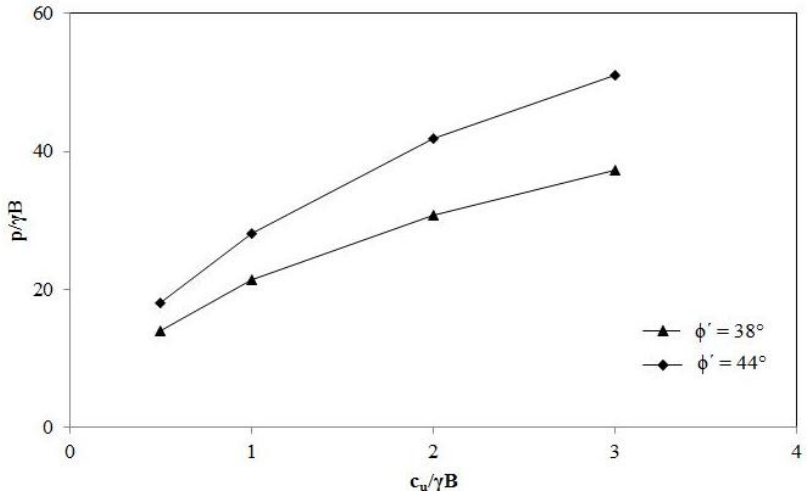

Fig. 13 The variation of $p/\gamma B$ with $c_u/\gamma B$ (H/B = 1.0, $q/\gamma B$ = 0)

Table 4 The $p/\gamma B$ values obtained from FE analyses in the cases of $\phi' = 38°$ and $\phi' = 44°$

$\phi' = 38°$			**$\phi' = 44°$**			**(%)**
H/B (m)	$c_u/\gamma B$	$P/\gamma B$	H/B (m)	$c_u/\gamma B$	$P/\gamma B$	
1.00	0.50	13.968	1.00	0.50	18.036	29.127
1.00	1.00	21.342	1.00	1.00	28.019	31.287
1.00	2.00	30.739	1.00	2.00	41.889	36.274
1.00	3.00	37.208	1.00	3.00	51.123	37.395

Where;
N_c; bearing capacity factor, N_c =5.14,
γ; unit weight of sand,
B; footing width,
L; footing length,
D; depth of the footing from the ground level,
H; the thickness of the sand layer as a distance between the footing base and surface of clay layer.

Hanna and Meyerhof (1980) have shown that in case of relatively weak clay layer compared to sand layer, passive failure of the sand may be accompanied by a failure surface that extends downwards into clay. In this case, passive earth pressure coefficient, K_P, value that is obtained by assuming the failure confined into sand layer, would be much higher. Therefore, Hanna and Meyerhof (1980) developed a new coefficient called Punching Shear Coefficient, K_S, to consider conveniently the passive force on a vertical plane beneath the footing edges. K_S is related with K_P by the equation $K_P \tan\delta = K_S \tan\phi'$. δ is inclination of the passive force P_P with the horizontal. Hanna and Meyerhof (1980) developed alternative design charts to define the coefficient of punching shear.

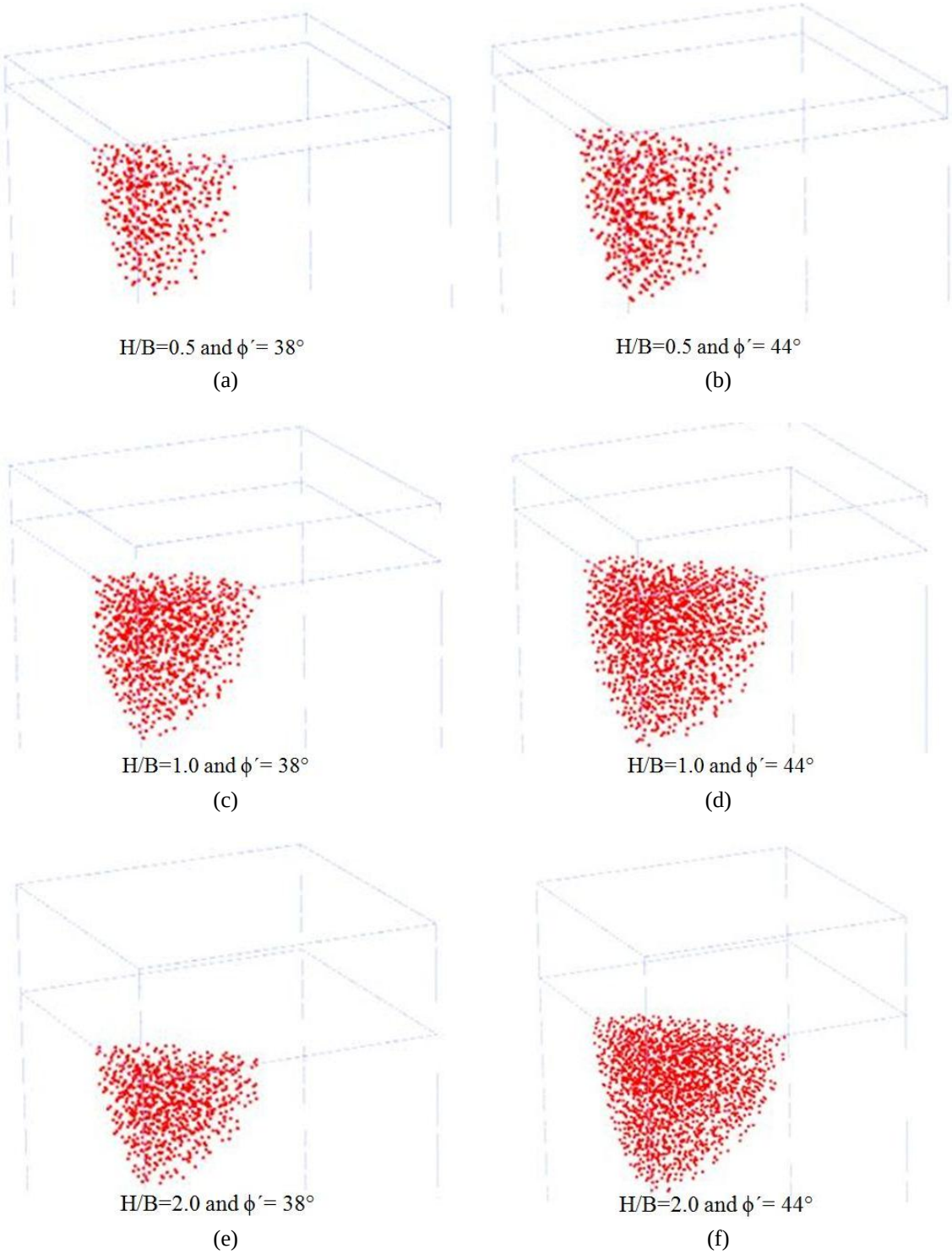

Fig. 14 The plastic failure zones occurring in clay layer for the cases of ϕ' = 38° and 44° ($c_u/\gamma B$ = 1.0, $q/\gamma B$ = 0)

Okamura *et al*. (1997) investigated ultimate bearing capacity, failure mechanism and deformation behavior associated with it, by performing a series of centrifuge model tests on dense sand overlying soft clay. Okamura *et al*. (1998) suggested a failure mechanism based on centrifuge test results. The following equation was obtained using the limit equilibrium method and offered for circular footings.

$$q_f = \left(1 + 2\frac{H}{B}tan\alpha_c\right)^2 \left(c_u N_c s_c + p_0^{'} + \gamma^{'} H\right)$$

$$+ \frac{4K_P sin\left(\emptyset^{'} - \alpha_c\right)}{cos\emptyset^{'} cos\alpha_c}\left\{\left(p_0^{'} + \frac{\gamma^{'} H}{2}\right)\frac{H}{B} + p_0^{'} tan\alpha_c \left(\frac{H}{B}\right)^2 + \frac{2}{3}\gamma^{'} H tan\alpha_c \left(\frac{H}{B}\right)^2\right\} \qquad (5)$$

$$- \frac{\gamma^{'} H}{3}\left\{4\left(\frac{H}{B}\right)^2 tan^2\alpha_c + 6\frac{H}{B}tan\alpha_c + 3\right\}$$

Where;

N_c; bearing capacity factor, N_c =5.1,
s_c; shape factor, s_c =1.2 for circular footings,
$\gamma^{'}$; effective unit weight of sand,
B; diameter of footing,
H; the thickness of the sand layer,
p'_0; effective overburden pressure at the footing base level.

In this failure mechanism, it was assumed that the vertical stress on the base of sand block is equal to the ultimate bearing capacity of a rigid footing with rough base on the clay subjected to a surcharge pressure. However, load spread angle in the upper sand layer changes with both strength parameters of layers and the thickness of upper sand layer.

In this paper, to calculate the bearing capacity of a square footing using the method proposed by Okamura *et al*. (1998), the base area of the square footing was converted to equivalent circular area.

Normalized bearing capacity, p/γB, values obtained from the FE analyses were compared with those from the limit equilibrium equations proposed by Meyerhof (1974) and Okamura *et al*. (1998). p/γB values were obtained for different H/B ratios ranging from 0.50 to 2.0 and c_u/γB values selected as 0.50 – 1.0 and 2.0. The results presented in Table 5.

As seen from Table 5, Meyerhof's results tend to underestimate the bearing capacity for all of the cases considered. Ultimate bearing capacities obtained from Meyerhof's method are nearly half of those estimated from FE method for all of the H/B ratios and value of c_u/γB = 0.50. The differences are averagely 45% and 40% for the c_u/γB values of 1.0 and 2.0, respectively. Therefore, Meyerhof' method is over safe.

The method proposed by Okamura *et al*. (1998) showed good agreement with the FE solutions up to H/B ≤ 1.0. For the H/B ratios higher than 1.0 the results become inconsistent. The values of the normalized bearing capacities obtained from the method by Okamura *et al*. (1998) are higher than the values estimated by FE method for the ratios of H/B > 1.0. The difference between p/γB values is 67% for the case of H/B = 1.50 and c_u/γB = 0.50. This ratio is averagely 39% for the cases of c_u/γB = 1.0 and 2.0. These methods have been developed when the punching shear effects are significant and cannot be neglected. Up to H/B < 1.50, punching shear seems to be effective and this effect diminishes for higher H/B ratios greater than 1.0.

Table 5 The comparison of the normalized bearing capacity (p/γB**)** values

$\phi' = 38°$			**Normalized bearing capacity values, p/γB**		
H/B	c_u/γB	q/γB	$(p/\gamma B)_{Meyerhof}$	$(p/\gamma B)_{Okamura\ et.\ al.}$	$(p/\gamma B)_{Plaxis\ 3D}$
0.50	0.50	0	3.851	6.882	7.620
	1.00		7.144	11.362	12.775
	2.00		13.521	20.286	21.748
0.75	0.50	0	4.810	10.439	10.394
	1.00		8.365	16.391	15.746
	2.00		15.003	26.905	23.553
1.00	0.50	0	6.152	17.049	13.968
	1.00		10.074	22.830	21.342
	2.00		17.078	35.590	30.739
1.50	0.50	0	9.988	35.780	21.368
	1.00		14.957	44.069	31.670
	2.00		23.006	60.223	43.204
2.00	1.00	0	21.793	76.026	38.256
0.50	1.00	1	11.074	20.037	20.892
1.00			18.887	41.434	30.805
1.50			27.676	73.558	43.246

The value of the ultimate bearing capacity could be significantly different depending on the limit equilibrium method used.

Table 5 presents the comparison of the values of normalized bearing capacities obtained from FE analyses and different methods based on limit equilibrium approach.

4.2 Surcharge effect

A series of FE analyses have been performed to investigate the surcharge effect on the bearing capacity of a sand layer overlying clay considering four different surcharge values such as q/γB = 0, 0.50, 1.0 and 2.0. The surcharge was modelled applying a constant uniform distributed pressure to the top boundary of surface elements equal to the considered magnitude of surcharge (Lee *et al*. 2005).

Fig. 15 shows the normalized bearing capacity-settlement curves obtained for different values of surcharge in the case of H/B = 1.0, c_u/γB = 1.0 and $\phi' = 38°$. As shown in Fig. 15, the normalized bearing capacity increases with increasing surcharge effect and the curves get stiffer. Plastic failure zones obtained from FE analyses for different values of q/γB in the case of H/B = 1.0, c_u/γB = 1.0 and $\phi' = 38°$ have been illustrated in Fig. 16. As surcharge effect increases, the failure zones within the lower clay extend more deeper by enlarging while in the upper sand layer, plastic failure zones are more intense and narrow.

When a surcharge exists, further variation of the friction angle with respect to the no-surcharge condition is expected. Because, surcharge increases the magnitude of confining stress acting on the upper sand layer located within the failure zone and causes mobilizing more of the available shear

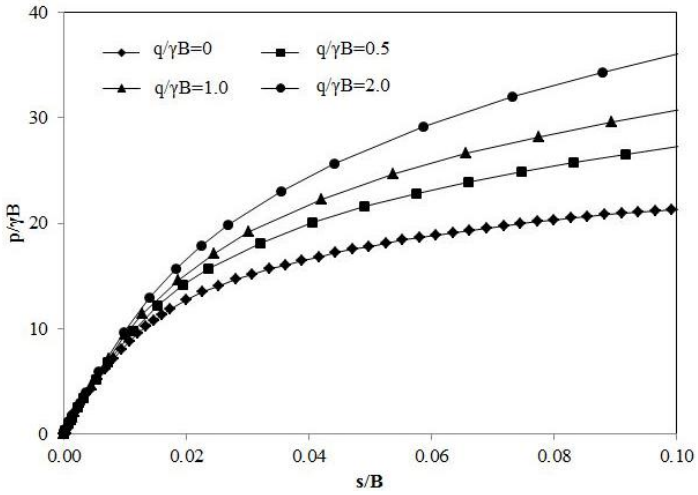

Fig. 15 The normalized bearing capacity-settlement curves with surcharge (H/B = 1.0, $c_u/\gamma B$ = 1.0, ϕ' = 38°)

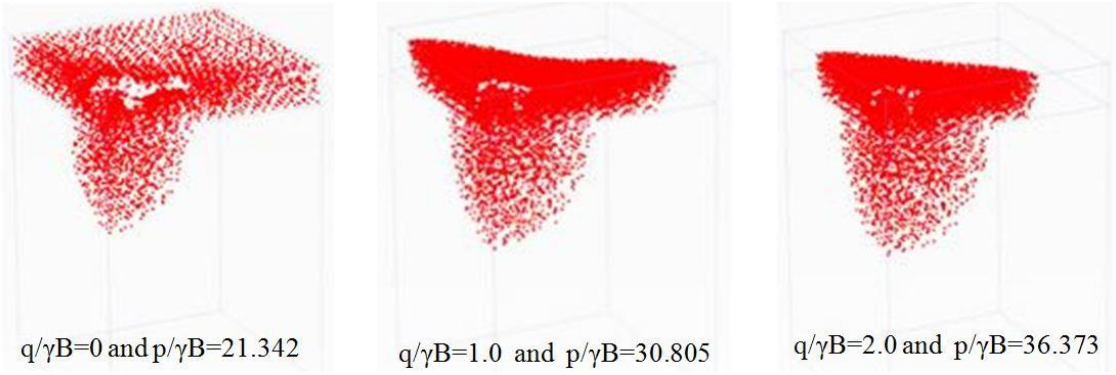

(a) (b) (c)

Fig. 16 The plastic failure zones obtained for different values of $q/\gamma B$ (H/B = 1.0, $c_u/\gamma B$ = 1.0, ϕ' = 38°)

resistance angle. In addition, dilatancy behavior of sand layer is suppressed due to the surcharge limits the upward movement of sand near the footing edge. These result in an increase in bearing capacity. However, the failure zones within the clay layer extend much deeper by enlarging because of the increasing overburden pressure on the clay surface including the weight of upper sand layer and surcharge. When the surcharge increases, the probability of occurrence of punching shear failure increases.

As seen from Fig. 17, the mechanism associated with failure of square footings, for the cases of H/B $\leq$ 1.50, suggests diagonal symmetry. However, the diagonal symmetry of the failure mechanism gets lost with H/B ratios greater than 1.50.

Although the $p/\gamma B$ increases with increasing $q/\gamma B$ for all of the H/B ratios considered, the growth of the $p/\gamma B$ is not linearly proportional to the increment of $q/\gamma B$. As seen from Table 6, the amount of increment in bearing capacity observed for the cases that $q/\gamma B$ increases from 1.0 to 2.0 increases with increasing H/B. As the depth of upper sand layer increases, the confining stress

effect of the surcharge pressure on the sand layer decreases. Therefore, increment in the bearing capacity decreases with increasing H/B ratio when the $q/\gamma B$ increases from 0 to 1.0. As shown in Table 7, the amount of increment in the $p/\gamma B$ values decreases with increasing $c_u/\gamma B$ when the $q/\gamma B$ increases from 1.0 to 2.0.

Table 6 The variation of $p/\gamma B$ with $q/\gamma B$ for different H/B values

H/B	$c_u/\gamma B$	$q/\gamma B$	$p/\gamma B$	**%**
0.50	1.00	0	12.775	63.538
		1.00	20.892	14.388
		2.00	23.898	
1.00		0	21.342	44.339
		1.00	30.805	18.074
		2.00	36.373	
2.00		0	38.257	40.868
		1.00	53.892	21.767
		2.00	65.623	

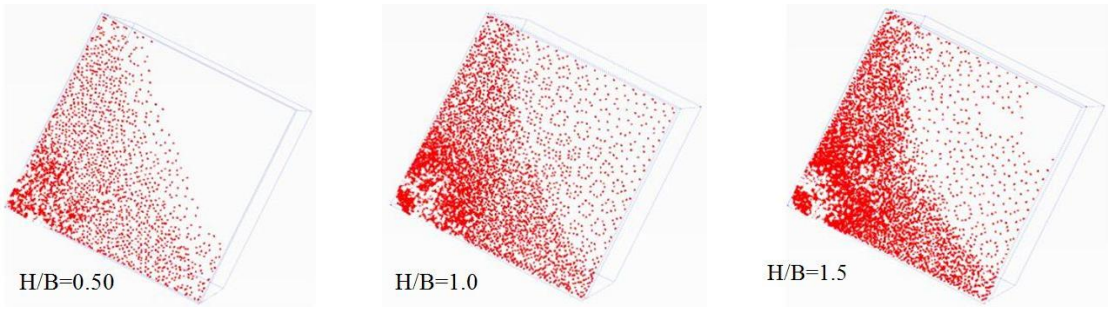

(a) (b) (c)

(d) (e)

Fig. 17 The variation of failure mechanism of square footings with H/B ratios ($c_u/\gamma B$ = 1.0 and ϕ' = 38°)

Table 7 The variation of $p/\gamma B$ with $q/\gamma B$ for different $c_u/\gamma B$ values

H/B	$c_u/\gamma B$	$q/\gamma B$	$p/\gamma B$	**%**
1.00	0.50	00	13.968	51.954
		1.00	21.225	
		2.00	26.613	25.38
	1.00	0	21.342	44.339
		1.00	30.805	
		2.00	36.373	18.074
	2.00	0	30.739	51.514
		1.00	46.574	
		2.00	53.227	14.284
	3.00	0	37.208	60.933
		1.00	59.880	
		2.00	66.534	11.112

5. Conclusions

The ultimate bearing capacity and failure mechanism of square footings on a sand layer overlying clay soil have been investigated numerically by performing a series of three-dimensional non-linear finite element analyses. Based on the investigation results following main conclusions can be drawn.

- The critical depth, $H/B_{critical}$, is not a constant value for the layered soils. It changes depending on both the strengths of upper sand layer and lower clay layer. Thus, for the cases of $c_u/\gamma B \leq 2.0$, the value of H/B ratio is equal to 3 while for the cases of $c_u/\gamma B > 2$ it is approximately $H/B \geq 1.50$. $H/B_{critical}$ decreases with increasing value of $c_u/\gamma B$. For the cases with H/B smaller than $H/B_{critical}$, $p/\gamma B$ increases with increasing $c_u/\gamma B$. The relationship between $p/\gamma B$ and $c_u/\gamma B$ is approximately linear in the cases of $H/B \leq 1$ while it is not linear for $H/B > 1$.
- The thickness of the upper sand layer (H), the undrained shear strength (c_u) of lower clay and the strength of sand (ϕ') are the most important parameters affecting the type of failure will occur. Increasing strength of upper sand layer increases the probability of punching shear type failure. As the thickness of upper sand layer greater than the footing width, it does not always mean that the failure zone is limited in the sand. When the bearing capacity of a sand layer overlying clay reaches that of the uniform sand it becomes independent of the $c_u/\gamma B$ value.
- The value of mobilized angle of internal friction can be assumed as equal to peak value for the cases $H/B > 2.0$. However, since the vertical stress increment on the surface of clay layer

decreases with increasing thickness of upper sand layer, the influence of clay layer on the bearing capacity and failure mechanism will be decreased with increasing H/B. Failure occurs depending on the bearing capacity of lower clay layer and the strength of sand is not efficient on failure behavior for the cases of $H/B \leq 1.0$.

- As the H/B increases, the surcharge effect on the clay layer increases. The surcharge clearly suppresses the upward movement of clay and forces the plastic failure zone to be much wider and deeper mobilizing more of the available shear strength of clay and provides a positive contribution to the bearing capacity. This behavior is more remarkable for the cases in which the governing criterion for the bearing capacity is undrained shear strength of clay. However; similar behavior could not be observed for the cases with H/B ratios ($H/B \geq 1.50$) in which the thickness of upper sand layer close to or greater than $H/B_{critical}$.
- Meyerhof's results tend to underestimate the bearing capacity for all of the cases considered. Ultimate bearing capacities obtained from Meyerhof's method are nearly half of those estimated from FE method for all of the H/B ratios and value of $c_u/\gamma B = 0.50$. The differences are averagely 45% and 40% for the $c_u/\gamma B$ values of 1.0 and 2.0, respectively. Therefore, Meyerhof' method is over safe.
- The method proposed by Okamura *et al*. (1998) showed good agreement with the FE solutions up to $H/B \leq 1.0$. For the H/B ratios higher than 1.0 the results become inconsistent. The values of the normalized bearing capacities obtained from the method by Okamura *et al*. (1998) are higher than the values estimated by FE method for the ratios of $H/B > 1.0$. The difference between $p/\gamma B$ values is 67% for the case of $H/B = 1.50$ and $c_u/\gamma B = 0.50$. This ratio is averagely 39% for the cases of $c_u/\gamma B = 1.0$ and 2.0.
- The methods based on limit equilibrium approach have been developed when the punching shear effects are significant and cannot be neglected. Up to $H/B < 1.50$, punching shear seems to be effective and this effect diminishes for higher H/B ratios greater than 1.0.
- The value of the ultimate bearing capacity could be significantly different depending on the limit equilibrium method used.
- The normalized bearing capacity increases with increasing surcharge effect and the load-settlement curves get stiffer. As surcharge effect increases, the failure zones within the lower clay extend deeper by enlarging while in the upper sand layer, plastic failure zones are more intense and narrow. Although the $p/\gamma B$ increases with increasing $q/\gamma B$ for all of the H/B ratios considered, the growth of the $p/\gamma B$ is not linearly proportional to the increment of $q/\gamma B$.
- The mechanism associated with failure of square footings, for the cases of $H/B \leq 1.50$, suggests diagonal symmetry. However, the diagonal symmetry of the failure mechanism gets lost with H/B ratios greater than 1.50.

References

Akpila, S.B. (2007), "The design of a shallow foundation on sand overlying soft clay", *Inter-World J. Sci. Technol.*, **3**(3), 21-26.

Amar, S., Baguelin, F., Canepa, Y. and Frank, R. (1994), "Experimental study of the settlement of shallow foundations", *Geot. Spec. Pub., ASCE*, **40**(2), 1602-1610.

Bandini, P. and Pham, H.V. (2011), "Bearing capacity of embedded strip footings in two-layered clay soils", *Geo-Frontiers 2011*, 332-341.

Baglioni, V.P., Chow, G.S. and Endley, S.N. (1982), "Jack-up foundation stability in stratified soil profiles", *Proceedings of the 14th Offshore Technology Conference*, Houston, TX, USA, May, Volume 4, pp. 363-369.

Benmebarek, S., Benmoussa, S., Belounar, L. and Benmebarek, N. (2012), "Bearing capacity of shallow foundation on two clay layers by numerical approach", *Geotech. Geol. Eng.*, **30**(4), 907-923.

Briaud, J-L. and Jeanjean, P. (1994), "Load settlement curve method for spread footings on sand", *J. Geotech. Geoenviron. Eng.*, **133**(8), 905-920.

Burd, H.J. and Frydman, S. (1997), "Bearing capacity of plane-strain footings on layered soils", *Can. Geotech. J.*, **34**(2), 241-253.

Cerato, A.B. (2005), "Scale effect of shallow foundation bearing capacity on granular material", Ph.D. Dissertation; University of Massachusetts Amherts, MA, USA.

Cerato, A.B. and Lutenegger, A.J. (2007), "Scale effect of shallow foundation bearing capacity on granular material", *J. Geotech. Geoenviron. Eng.*, **133**(10), 1192-1202.

Florkiewicz, A. (1989), "Upper bound to bearing capacity of layered soils", *Can. Geotech. J.*, **26**(4), 730-736.

Gourvenec, S., Randolph, M. and Kingsnorth, O. (2006), "Undrained bearing capacity of square and rectangular footings", *Int. J. Geomech.*, **6**(3), 147-157.

Hanna, A.M. (1981), "Foundations on strong sand overlying weak sand", *J. Geotech. Eng. Div.*, **107**(7), 915-927.

Hanna, A.M. and Meyerhof, G.G. (1980), "Design charts for ultimate bearing capacity of foundations on sand overlying soft clay", *Can. Geotech. J.*, **17**(2), 300-303.

Huang, M. and Qin, H.L. (2009), "Upper-bound multi-rigid-block solutions for bearing capacity of two-layered soils", *Comput. Geotech.*, **36**(3), 525-529.

Jahanandish, M., Veiskarami, M. and Ghahramani, A. (2010), "Effect of stress level on the bearing capacity factor, N_γ, by the ZEL method", *KSCE J. Civil Eng.*, **14**(5), 709-723.

Jaky, J. (1944), "The coefficient of earth pressure at rest", *J. Soc. Hungarian Archit. Eng.*, **78**(22), 355-358.

Kenny, M.J. and Andrawes, K.Z. (1997), "The bearing capacity of footings on a sand layer overlying soft clay", *Geotechnique*, **47**(2), 339-345.

Kraft, L.M. and Helfrich, S.C. (1983), "Bearing capacity of shallow footing, sand over clay", *Can. Geotech. J.*, **20**(1), 182-185.

Kumar, J. and Kouzer, K.M. (2007), "Effect of footing roughness on bearing capacity factor, N_γ", *J. Geotech. Geoenviron. Eng.*, **133**(5), 502-511.

Lavasan, A.A. and Ghazavi, M. (2012), "Behavior of closely spaced square and circular footings on reinforced sand", *Soil. Found.*, **52**(1), 160-167.

Lee, J., Salgado, R. and Kim, S. (2005), "Bearing capacity of circular footings under surcharge using state-dependent finite element analysis", *Comput. Geotech.*, **32**(6), 445-457.

Merifield, R.S. and Nguyen, V.Q. (2006), "Two and three-dimensional bearing capacity solutions for footings on two-layered clays", *Geomech. Geoeng.: Int. J.*, **1**(2), 151-162.

Merifield, R.S., Sloan, S.W. and Yu, H.S. (1999), "Rigorous plasticity solutions fort he bearing capacity of two-layered clays", *Geotechnique*, **49**(4), 471-490.

Meyerhof, G.G. (1974), "Ultimate bearing capacity of footings on sand overlying clay", *Can. Geotech. J.*, **11**(2), 223-229.

Michalowski, R.L. and Shi, L. (1995), "Bearing capacity of footings over two-layer foundation soils", *J. Geotech. Eng.*, **121**(5), 421-428.

Okamura, M., Takemura, J. and Kimura, T. (1997), "Centrifuge model tests on bearing capacity and deformation of sand layer overlying clay", *Soil. Found.*, **37**(1), 73-88.

Okamura, M., Takemura, J. and Kimura, T. (1998), "Bearing capacity predictions of sand overlying clay based on limit equilibrium methods", *Soil. Found.*, **38**(1), 181-194.

Plaxis 3D (2012), Delft, Netherlands.

Purushothamaraj, P., Ramiah, B.K. and Rao, K.N.V. (1974), "Bearing capacity of strip footings in two layered cohesive-friction soils", *Can. Geotech. J.*, **11**(1), 32-44.

Shiau, J.S., Lyamin, A.V. and Sloan, S.W. (2003), "Bearing capacity of a sand layer on clay by finite element limit analysis", *Can. Geotech. J.*, **40**(5), 900-915.

Taiebat, H.A. and Carter, J.P. (2000), "Numerical studies of the bearing capacity of shallow foundations on cohesive soil subjected to combined loading", *Geotechnique*, **50**(4), 409-418.

Terzaghi, K. (1943), *Theoretical Soil Mechanics*, Wiley, New York, NY, USA.

Yamaguchi, H. (1963), "Practical formula of bearing value for two layered ground", *Proceedings of the 2nd Asian Regional Conference on SMFE*, Tokyo, Japan, May, Volume 1, pp. 176-180.

Yamaguchi, H. and Terashi, M. (1971), "Ultimate bearing capacity of multi-layered ground", *Proceedings of the 4th Asian Regional Conference on SMFE*, Bangkok, Thailand, July-August, Volume 1, pp. 99-105.

Yamamoto, K. and Kim, D. (2004), "Bearing capacity of spread foundations on sand overlying clay", *Lowland Technol. Int.*, **6**(2), 33-45.

Yu, L., Liu, J., Kong, X. and Hu, Y. (2011), "Three-dimensional large deformation FE analysis of square footings in two-layered clays", *J. Geotech. Geoenviron. Eng.*, **137**(1), 52-58.

Yuan, F.F. and Luan, M.T. (2005), "Study on bearing behaviors of foundations on multi-layer subsoil", *Proceedings of the International Symposium on Frontiers in Offshore Geotechnics*, Perth, WA, Australia, September, pp. 19-21.

GC